Thermally induced evolution of optical and structural properties of Er2O3 films grown on Si substrates by thermal atomic layer deposition

L. Khomenkova, M.-P. Chauvat, P. Marie, C. Frilay, Franck Lemarié, S. Boudin, X. Portier, Nicolas Ratel-Ramond, Christophe Labbe, J. Cardin, et al.

▶ **To cite this version:**

L. Khomenkova, M.-P. Chauvat, P. Marie, C. Frilay, Franck Lemarié, et al.. Thermally induced evolution of optical and structural properties of Er2O3 films grown on Si substrates by thermal atomic layer deposition. Materials Letters, 2020, 263, pp.127216. 10.1016/j.matlet.2019.127216 . hal-02424202

HAL Id: hal-02424202
https://hal.science/hal-02424202v1

Submitted on 23 Mar 2020

HAL is a multi-disciplinary open access archive for the deposit and dissemination of scientific research documents, whether they are published or not. The documents may come from teaching and research institutions in France or abroad, or from public or private research centers.

L'archive ouverte pluridisciplinaire **HAL**, est destinée au dépôt et à la diffusion de documents scientifiques de niveau recherche, publiés ou non, émanant des établissements d'enseignement et de recherche français ou étrangers, des laboratoires publics ou privés.

Thermally induced evolution of optical and structural properties of Er_2O_3 films grown on Si substrates by thermal atomic layer deposition

L. Khomenkova [a,*], M.-P. Chauvat [a], P. Marie [a], C. Frilay [a], F. Lemarié [a], S. Boudin [b], X. Portier [a], N. Ratel-Ramond [c], C. Labbé [a], J. Cardin [a], F. Gourbilleau [a]

[a] CIMAP, Normandie Univ, ENSICAEN, UNICAEN, CEA, CNRS, 6 Boulevard Maréchal Juin, 14050 Caen Cedex 4, France
[b] CRISMAT, Normandie Univ, ENSICAEN, UNICAEN, CNRS, 6 Boulevard Maréchal Juin, 14050 Caen Cedex 4, France
[c] CEMES/CNRS, 29 rue Jeanne Marvig, 31055 Toulouse Cedex 4, France

Keywords:
Er_2O_3
Crystal structure
Electron microscopy
Thin films
Luminescence
FTIR

A B S T R A C T

Thermally induced evolution of structural and optical properties of Er_2O_3 films prepared by atomic layer deposition was investigated. The films were grown on Si substrates by water-assisted approach from (tris (methylcyclopentadienyl)erbium(III). As-deposited films showed cubic Er_2O_3 phase, and compressive stress. Isochronal (30 min) heating at 600–1100 °C in nitrogen flow caused strain relaxation, decrease of the lattice parameters and the increase of coherent domain size. Besides, in the films annealed at 1000–1100 °C, the formation of Er silicate phase was observed. This phase formed due to Si diffusion from substrate in film volume, and the presence of Si was found not only at the film/substrate interface, but also on the top surface of the film. This fact was explained by spinodal decomposition of Er silicate with the formation of Er_2SiO_5 phase on top surface. It was shown that both oxygen vacancies and Er^{3+} ions contribute to light emission, however, no energy transfer from vacancies to Er^{3+} ions was detected.

1. Introduction

Nowadays, more and more attention is paid to erbium oxide films owing to their applications in microelectronics [1,2], photonics [3], as well as protective and anticorrosion coatings [4]. Physical and chemical vapor deposition [3,5,6], sol–gel method [7], magnetron sputtering [8] are used for film growth. In recent years, atomic layer deposition (ALD) becomes more attractive. However, only a few groups reported on the successful fabrication of Er_2O_3 films [2,9,10,11]. In this work, we report on the effect of high-temperature annealing on optical and structural properties of Er_2O_3 films grown by water-assisted ALD approach.

2. Experimental details

Er_2O_3 films were grown on p-type Si substrates in a Picosun® 200 Advanced ALD tool using (tris(methylcyclopentadienyl)erbium(III) ($Er(CpMe)_3$, CAS No. 39740–10-5) as precursor and water as oxidant. During deposition, the substrate was kept at 300 °C and $Er(CpMe)_3$ was heated at 170 °C. The $Er(CpMe)_3/H_2O$ pulse/purge time sequence was 1.6 s/2.0 s/0.1 s/2.0 s. The film thickness was about 170 nm. After deposition, the substrates were cut into samples that were submitted to isochronal (30 min) annealing at T_A ranging from 500 to 1100 °C in nitrogen flow. The samples were studied at room temperature by means of Spectroscopic Ellipsometry, Fourier Transform Infrared (FTIR) spectroscopy, Photoluminescence (PL), X-Ray Diffraction (XRD), Atomic Force Microscopy (AFM), Transmission Electron Microscopy (TEM) and Energy-Dispersive X-Ray spectroscopy (EDX) methods. More details about experimental methods are given in the supplement section.

3. Experimental results and discussion

3.1. Evolution of refractive index and film thickness with T_A

As-deposited films demonstrated the refractive index n = 1.85 9–1.861 (at 1.95 eV) similar to that reported for Er_2O_3 in Refs. [12,13]. Thermal treatment results in its non-monotonic variation (Fig. 1,a, Fig. 1S). The T_A increase up to 700 °C causes the n rising up to 1.952–1.956 (at 1.95 eV) along with some thickness decrease, which testifies to the film crystallization and densification. Further T_A rising causes the n decrease down to 1.935–1.937 (Fig. 1,a) due to the formation of the phase with lower refractive index, for

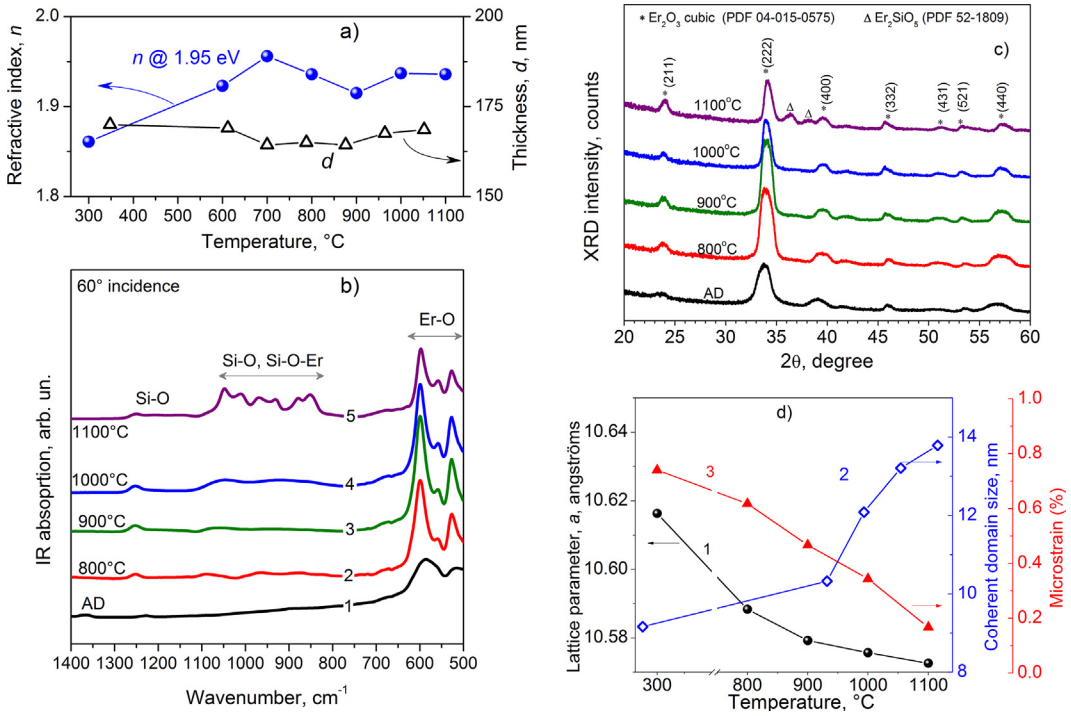

Fig. 1. Effect of annealing temperature on: a) refractive index and thickness of the films; b) FTIR spectra (recorded with 60° incidences of excitation light); c) grazing-incidence XRD patterns (ω = 0.5°; Co $K_{\alpha,\lambda}$ = 1.78897 Å); d) lattice parameter (1), coherent domain size (2) and microstrain (3). The curves in b) and c) are shifted vertically for clarity. The data at T_A = 300 °C in d) correspond to as-deposited film.

instance, some pores or cavities or SiO_x and Er silicate phases. The analysis of absorption spectra (Fig. 1S,d), using general Tauc model and assuming Er_2O_3 films as allowed transitions indirect bandgap material similar to Ref. [13], showed that the annealing results in some decrease of bandgap value from E_g = 5.28 eV (as-deposited films) down to E_g = 4.95 eV (T_A = 1100 °C) (Fig. 1S,d). This E_g behavior is the evidence of the formation of Er silicate phase in the films.

3.2. Evolution of FTIR spectra and XRD patterns with T_A

The FTIR spectra of as-deposited films showed Er-O vibration band in the 400–650 cm^{-1} range (Fig. 1,b) and OH-vibration band in the 3200–3600 cm^{-1} range (not shown here). This band is due to the presence of residual OH groups in the film after deposition. An annealing at T_A = 500–600 °C caused desorption of OH groups only. For T_A = 700–1100 °C, instead of broad Er-O band some resolved peaks appear, being sharper for higher T_A (Fig. 1,b). Besides, additional Si-O bands at 1250, 1080 and 820 cm^{-1} along with the Si-O-Er vibration bands were observed (Fig. 1,b) that can be explained by Si diffusion in the film volume.

Grazing-incidence XRD data supports these findings (Fig. 1,c). As-deposited films grown at 300 °C were already crystallized in the cubic Er_2O_3 phase (PDF No. 04-015-0575). The most intense peaks in the 2θ = 20-60° range were found at 2θ = 23.48° (2 1 1), 33.73° (2 2 2), 39.10° (4 0 0) and 56.82° (4 4 0) (Fig. 1,c), being shifted to lower angles in comparison with standard values. This shift is caused by mismatching in lattice parameters of the film and substrate. Indeed, for standard Er_2O_3, the a_{Er2O3} = 1.054 nm value is close to twice the unit cell of Si substrate ($2a_{Si}$ = 1.086 nm). However, small negative mismatch for the Er_2O_3 generated its stress. For as-deposited films, it was found that a_{Er2O3} = 1.0617 nm and the microstrains are ~0.74% (Fig. 1,d).

A supplementary annealing leads to further film crystallization and strain relaxation. Indeed, the T_A increase up to 1000 °C gives rise to some narrowing of XRD peaks and the gradual shift towards higher angles, i.e. 2 θ = 24.06° (2 1 1), 34.12° (2 2 2), 39.64° (4 0 0) and 57.36° (4 4 0) (Fig. 1,c), approaching the values of standard cubic Er_2O_3. The highest intensity of the peak at 2 θ = 33.73° (2 2 2) is the evidence of the preferable orientation of the film following the [1 1 1] direction. The analysis of XRD data revealed the gradual decrease of the lattice parameters down to 1.057 nm and the increase of coherent domain size from ~9 nm up to ~14 nm as well as stress relaxation down to 0.17% (Fig. 1,d). No any other Er_2O_3 phases were distinguished in the annealed films, whereas for T_A = 1100 °C, additional XRD peaks appeared at 2 θ = 35.36° and 38.15° (Fig. 1,c) that can be assigned to Er_2SiO_5 phase (PDF card No. 52-1809).

3.3. Study of the films with microscopy methods

Analysis of the surface of the same samples confirmed the formation of some grains (Fig. 2S and 3S) and appearance of some cracks at T_A = 900–1100 °C supporting the statement on the stress relaxation. It should be noted that not only mismatching in lattice parameters, but also the presence of OH-groups could be the reasons of this phenomenon.

To obtain information on spatial localization of SiO_x and/or Er silicate phases in the samples annealed at 1000 and 1100 °C, their cross-sectional specimens were observed using TEM method. It was confirmed that the Er_2O_3 grains have cubic structure. An example is shown in Fig.2, where a grain is oriented following a [1 1 1] direction (Fig. 2). Some cavities were found in the film volume and their amount increases for higher T_A. The interfacial layers with thicknesses of 18 nm (T_A = 1000 °C) and 23.5 nm (T_A = 1100 °C) were observed.

The EDX analyses confirmed that this layer is Er silicate (Table 1). Si atoms are distributed over the whole film annealed at 1100 °C. However, Si content is significant only in the interfacial layer and at the film surface. This result showed that high-temperature annealing stimulates Si diffusion from the substrate

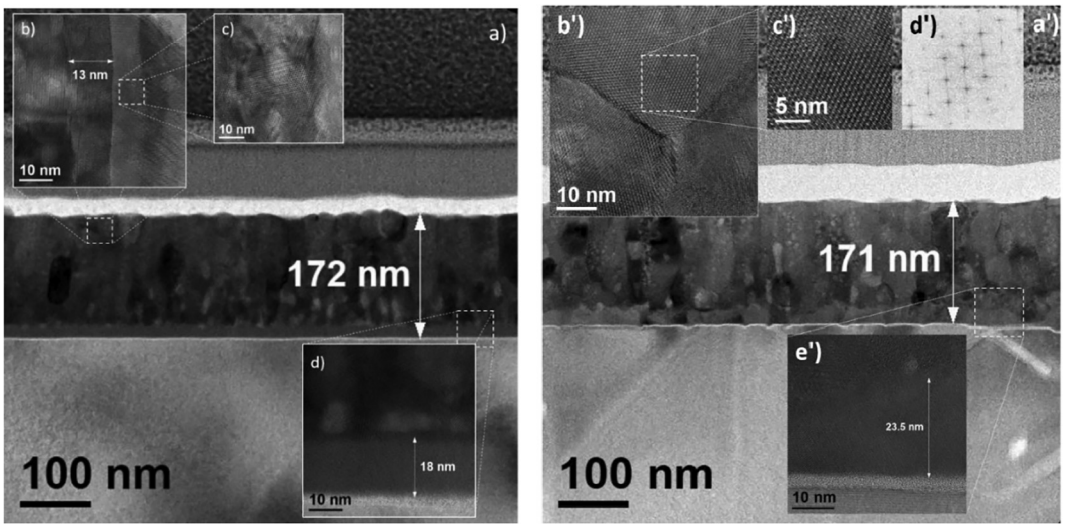

Fig. 2. Bright field TEM (a, a'), high-resolution TEM images (b–d, b', c', e') and selected FFT (d') of cross-section of Er_2O_3 films annealed at 1000 °C (a–d) and 1100 °C (a'–e').

Table 1
Chemical composition of the films annealed at 1000 and 1100 °C (Fig. 2).

Annealing temperature	Zone of the sample	Chemical composition		
		Er, at.%	O, at.%	Si, at.%
1000 °C (Fig. 2, a–d)	Interfacial layer	22.5	60.8	16.7
	Film volume	42.8	56.5	0.4
1100 °C (Fig. 2, a'–e')	Interfacial layer	22.3	68.4	10.3
	Film volume	35.9	63.1	1.0
	Near surface region	19.4	71.0	9.6

to the film volume followed by formation of Er silicate phase. However, this phase tends to decompose followed by preferential Si segregation at the film/substrate and film/air interfaces. The formation of Er_2SiO_5 phase and further crystallization of Er_2O_3 grains occur.

3.4. PL properties of the films

Fig. 3,a shows PL spectra recorded under "resonant" excitation (532 nm corresponding to Er^{3+} absorption in the $^4I_{15/2}\rightarrow{}^4H_{11/2}$ transition). Two main bands due to the $^4F_{9/2}\rightarrow{}^4I_{15/2}$ (650–700 nm) and $^4I_{9/2}\rightarrow{}^4I_{15/2}$ (780–830 nm) are seen. In the as-deposited films, the Er^{3+} related peaks are broad testifying some disorder in film volume. Annealed films (T_A = 800–900 °C) showed sharp Er^{3+} peaks (Fig. 3,a) that confirm the presence of Er ions in crystalline host. Further T_A rise results in the appearance of broad PL bands peaked near 620 and 700 nm, being overlapped with Er^{3+} PL bands (Fig. 3). The comparison of the evolution of structural and PL properties allowed assuming that these broad PL components are due to Er silicate phase formation.

To investigate the potential energy transfers from host defects to Er^{3+} ions, PL spectra were recorded also under non-resonant (350 nm) and resonant (378 nm, corresponding to $^4I_{15/2}\rightarrow{}^4G_{11/2}$ absorption for Er^{3+} ions) excitation. It turned out that under excitation with 350 nm light, the PL spectrum is broad and featureless (Fig. 3b), due to carrier recombination via the host defects such as oxygen vacancies. At the same time, under 378-nm excitation, sharp peaks related to Er^{3+} PL emission appeared. Thus, both host defects such (as oxygen vacancies) and Er^{3+} ions contribute to light emission, whereas no energy transfer from oxygen vacancies to Er ions was found.

4. Conclusions

The effect of annealing treatment on structural and optical properties of Er_2O_3 films was studied. Only cubic Er_2O_3 phase was detected in as-deposited films and in those annealed at T_A < 900 °C. Annealing at T_A = 900–1100 °C stimulates formation of Si-rich amorphous interfacial layer, whereas at T_A = 1100 °C, Er silicate phase (consistent with Er_2SiO_5) appeared on film surface

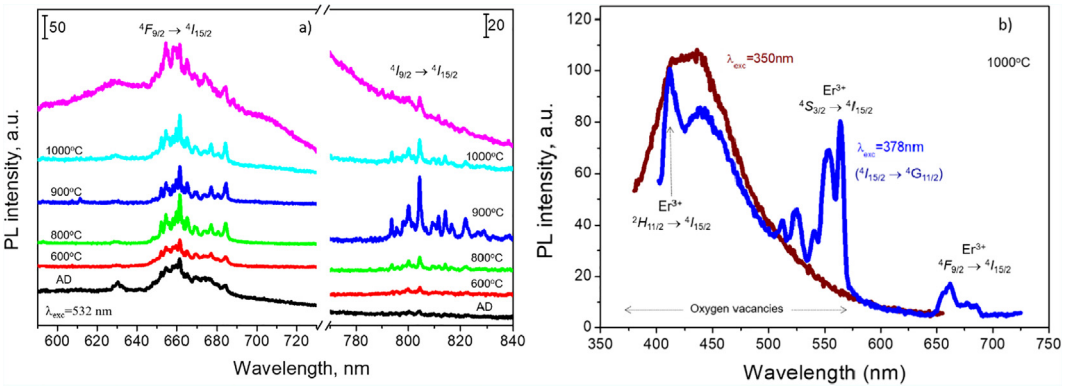

Fig. 3. a) Evolution of PL spectra of Er_2O_3 films with T_A. Excitation light wavelength is 532 nm. The spectra are shifted in vertical direction for clarity. b) PL spectra of the film annealed at 1000 °C recorded under non-resonant (350 nm) and resonant (378 nm) excitations.

due to Si diffusion from substrate. Both host defects (like oxygen vacancies) and Er^{3+} ions brought contributions to PL emission.

CRediT authorship contribution statement

L. Khomenkova: Conceptualization, Methodology, Investigation, Data curation, Writing - original draft, Writing - review & editing. **M.-P. Chauvat:** Data curation, Investigation, Visualization, Writing - review & editing. **P. Marie:** Data curation, Formal analysis, Visualization, Writing - review & editing. **C. Frilay:** Resources, Writing - review & editing. **F. Lemarié:** Resources, Writing - review & editing. **S. Boudin:** Resources, Writing - review & editing. **X. Portier:** Data curation, Investigation, Visualization, Validation, Writing - review & editing. **N. Ratel-Ramond:** Data curation, Investigation, Visualization, Validation, Writing - review & editing. **C. Labbé:** Investigation, Validation, Writing - review & editing. **J. Cardin:** Investigation, Formal analysis, Visualization, Validation, Writing - review & editing. **F. Gourbilleau:** Supervision, Project administration, Validation, Writing - review & editing.

Declaration of Competing Interest

The authors declare that they have no known competing financial interests or personal relationships that could have appeared to influence the work reported in this paper.

Acknowledgements

This work was supported by the Normandie Region and the "Fond Européen de Développement Régional" (FEDER) via LUMIERE project. XP is grateful to the "Agence Nationale de la Recherche" (ANR, France) for the EQUIPEX "GENESIS" grant "ANR-11-EQPX-0020" in the frame of the "Investissements d'avenir" as well as to the "Fond Européen de Développement Régional" (FEDER) and the Normandie Region for funding that allowed the purchase and the use of the FIB system for TEM sample preparations.

References

[1] V. Mikhelashvili, G. Eisenstein, F. Edelmann, J. Appl. Phys. 90 (2001) 5447–5449.
[2] M. Losurdo, M.M. Giangregorio, G. Bruno, D. Yang, E.A. Irene, A.A. Suvorova, M. Saunders, Appl. Phys. Lett. 91 (2007) 091914.
[3] S. Saini, K. Chen, X. Duan, J. Michel, L.C. Kimerling, M. Lipson, J. Electron. Mater. 33 (2004) 809–814.
[4] K.M. Hubbard, B.F. Espinoza, Thin Solid Films 366 (2000) 175–180.
[5] T.-M. Pan, C.-L. Chen, W.W. Yeh, S.-J. Hou, Appl. Phys. Lett. 89 (2006) 222912.
[6] M.P. Singh, C.S. Thakur, K. Shalini, N. Bhat, S.A. Shivashankar, Appl. Phys. Lett. 83 (2003) 2889–2891.
[7] Y.-H. Chang, M.-H. Chou, T.-J. Wang, Ceram. Intern. 44 (2018) 1163–1167.
[8] M. Miritello, R. Lo Savio, F. Iacona, G. Franzò, C. Bongiorno, A. Irrera, F. Priolo, J. Lumin. 121 (2006) 233–237.
[9] J. Päiväsaari, M. Putkonen, T. Sajavaara, L. Niinistö, J. Alloys Compounds 374 (2004) 124–128.
[10] P.-Y. Chen, A.B. Posadas, S. Kwon, Q. Wang, M.J. Kim, A.A. Demkov, J.G. Ekerdt, J. Appl. Phys. 122 (2017) 215302.
[11] K. Xu, A.R. Chaudhuri, H. Parala, D. Schwendt, T. de los Arcos, H.J. Osten, A. Devi, J. Mater. Chem. C 1 (2013) 3939–3946.
[12] G. Adachi, N. Imanaka, Chem. Rev. 98 (1998) 1479–1514.
[13] H.S. Kamineni, V.K. Kamineni, R.L. Moore, S. Gallis, A.C. Diebold, M. Huang, A.E. Kaloyeros, J. Appl. Phys. 111 (2012) 013104.